HHS Public Access

Author manuscript

Cancer Immunol Res. Author manuscript; available in PMC 2020 January 01.

Published in final edited form as:

Cancer Immunol Res. 2019 January ; 7(1): 50–61. doi:10.1158/2326-6066.CIR-18-0395.

High-throughput stability screening of neoantigen/HLA complexes improves immunogenicity predictions

Dylan T. Blaha[#1], **Scott D. Anderson**[#1], **Daniel M. Yoakum**[1], **Marlies V. Hager**[1], **Yuanyuan Zha**[2], **Thomas F. Gajewski**[2], and **David M. Kranz**[1,*]

[1]Department of Biochemistry, University of Illinois, Urbana, IL 61801, USA

[2]Department of Pathology, Department of Medicine, and the Ben May Department of Cancer, University of Chicago, Chicago, IL 60615, USA

[#] These authors contributed equally to this work.

Abstract

Mutated peptides (neoantigens) from a patient's cancer genome can serve as targets for T-cell immunity, but identifying which peptides can be presented by an MHC molecule and elicit T cells has been difficult. Although algorithms that predict MHC binding exist, they are not yet able to distinguish experimental differences in half-lives of the complexes (an immunologically relevant parameter, referred to here as kinetic stability). Improvement in determining actual neoantigen peptide/MHC stability could be important, as only a small fraction of peptides in most current vaccines are capable of eliciting $CD8^+$ T-cell responses. Here, we used a rapid, high-throughput method to experimentally determine peptide/HLA thermal stability on a scale that will be necessary for analysis of neoantigens from thousands of patients. The method combined the use of UV-cleavable peptide/HLA class I complexes and differential scanning fluorimetry (DSF) to determine the T_m values of neoantigen complexes. Measured T_m values were accurate and reproducible and were directly proportional to the half-lives of the complexes. Analysis of known HLA-A2–restricted immunogenic peptides showed that T_m values better correlated with immunogenicity than algorithm-predicted binding affinities. We propose that temperature stability information can be used as a guide for the selection of neoantigens in cancer vaccines in order to focus attention on those mutated peptides with the highest probability of being expressed on the cell surface.

Keywords

neoantigen; major histocompatibility complex; differential scanning fluorimetry; protein complex stability; half-life

[*]Correspondence should be addressed to David M. Kranz. (D.M.K.): Mailing Address: 600 S. Mathews Ave, Urbana, IL, 61801, Phone: (217)-244-2821, Fax: (217)244-5858, d-kranz@illinois.edu.

Author Contributions

S.D.A. and D.M.K. conceptualized the method; D.T.B., S.D.A., and D.M.Y. performed the experiments; D.T.B., S.D.A., D.M.Y., M.V.H. and D.M.K. analyzed the data; Y.Z. and T.J.G. provided peptides from inflamed and non-inflamed tumor samples and analyzed the results with these samples; and D.T.B., M.V.H. and D.M.K. wrote the manuscript with input from all of the authors.

Conflict of Interest: The authors declare that they have no conflicts of interest with this article.

Introduction

Successes in cancer immunotherapy have revealed that cancer neoantigens are the primary target for tumor reactive lymphocytes isolated from patients receiving checkpoint blockade therapy, such as anti–CTLA-4 and anti–PD-1 (1,2). This finding, coupled with breakthroughs in sequencing technology, has spurred interest in neoantigens as a source of therapeutic targets (3–7). Because each cancer evolves along unique pathways, principles of individualized medicine must be applied to the pursuit of neoantigens as therapeutic targets (8). This includes whole exome sequencing (WES) and RNA sequencing to determine a list of mutated peptides that could potentially serve as epitopes for immune recognition. From here, candidate neoantigen peptides are assessed using algorithms that predict their likelihood of proteosomal processing and their binding affinity for HLA molecules. Many protocols end the preliminary analysis here, and move straight into screening for T-cell immunogenicity or vaccine testing.

Studies from Buus and colleagues (9), and Schumacher and colleagues (10) suggest that the half-life of the ternary peptide-MHC (pepMHC) complex is a better indicator of immunogenicity than binding affinity. The half-life is determined from the dissociation kinetics of the complex, and can, thus, be considered a measure of the kinetic stability of the complex. Most kinetic stability and binding affinity studies have been done with the common HLA allele, HLA-A2. Predictions for this allele are likely to be the most accurate when it comes to class I MHC binding algorithms such as NetMHC4.0. In the study by Stronen et al. (10), 19% of the top 57 neoantigen peptides chosen based on NetMHC4.0 binding predictions were immunogenic. Based on experimental measurement of dissociation rates (using anti-β2m as a probe), the percent of immunogenic peptides increased to 50% of peptides with half-lives greater than 5 hours.

The ability to improve selection of appropriate neoantigen candidates is important, given the increasing interest in the use of peptides in vaccines (11). Two studies in melanoma patients (12,13), one using a peptide formulation and the other a mini-gene RNA vaccine, showed a relatively low frequency of $CD8^+$ T-cell responsiveness (16% and 29% of peptides in these studies, respectively). Because only a small fraction of a patient's neoantigen repertoire (approximately 10 to 20 neoantigen peptides) is typically selected for use in these vaccine trials, even a two-fold improvement in peptide candidate selection could be significant in terms of eliciting tumor immunity in patients.

Although the measurement of pepMHC dissociation rates (half-lives) provides an approach to determining the kinetic stability of the complexes, it is tedious, time-consuming, and not amenable to high throughput. To develop a rapid system with high-throughput capabilities, we reasoned that temperature stability should correlate with dissociation rates of the complexes. If so, a method exists that would be available to many labs because it uses a standard real-time (RT)-PCR instrument to determine temperature denaturation curves and stability, characterized by T_m, the temperature yielding half-maximal denaturation. The method, called differential scanning fluorimetry (DSF), relies on the binding of a commercially available fluorescent probe, SYPRO Orange, to denatured proteins (14).

Fluorescence is monitored in an RT-PCR instrument, where use of 384-well plates allows hundreds of complexes to be analyzed in a one-hour, hands-free experiment.

Here, we developed a strategy that allows crude peptide preparations to be used together with HLA-A2 and UV-peptide cleavage reactions, followed by DSF. We measured the thermal stability of many previously published HLA-A2 binding peptides for which half-life measurements, and in some cases, binding affinity measurements, were reported. We also compared T_m values and half-lives for a collection of self-peptides and single amino acid variants for which we determined half-lives using anti-β2m or soluble high-affinity T-cell receptor as probes. T_m values of the self-peptides and neoantigen peptides were then compared to binding affinities predicted using current algorithms. We found that thermal stabilities (T_m values) were correlated with half-life measurements, but less correlated with predicted binding affinities, and in some cases, less correlated with measured binding affinities. DSF provides a faster, simpler, and lower-cost alternative to half-life measurements and can be used to screen thousands of potential class I-restricted neoantigens rapidly.

Materials and Methods

Peptides.

Peptides were synthesized by GenScript (Piscataway, NJ) or Cellmano Biotech (Hefei, China). Sequences of GenScript peptides are shown in Table 1 and Supplementary Tables S1-S6, and sequences of Cellmano Biotech peptides are shown in Supplementary Tables S7 and S8. Peptides were provided either as ‘crude’ preparations for 96-well libraries (≥30% purity) or as preparations that were purified by HPLC (≥90% purity). Lyophilized peptides were suspended in dimethyl sulfoxide (DMSO) at a working concentration of 20 mM and stored at –20°C. Prior to use in peptide exchange reactions, peptides were incubated at 37°C for one hour.

Predicted peptide binding affinities for HLA-A2.

Peptide binding analyses were done using NetMHC 4.0 (an Artificial Neural Network (ANN), produced by the Technical University of Denmark, in which, results are expressed as predicted equilibrium binding constants (in nM) (15).

Generation of peptide/HLA-A2 complexes by UV-peptide exchange.

HLA-A*02:01 heavy chain and β2-microglobulin (β2m) were each expressed in *E.* coli strain BL21 and refolded from inclusion bodies, together with UV-photocleavable peptide (KILGFVF**J**V, where J represents the cleavable 3-amino-3-(2-nitro) phenyl-propionic acid) as described previously (16,17). Briefly, 3 mmol of heavy chain and 2 mmol β2m inclusion bodies were solubilized in 8 M urea (Fisher Scientific, BP-169–212) and refolded in the dark at 4°C together with 30 mg of UV-peptide in a 1 L folding reaction. UV-peptide HLA-A2 monomers were concentrated using an Amicon Stirred Ultrafiltration Cell with a 10,000 Da MWCO ultracentrifugation disk and dialyzed overnight using a 10,000 Da MWCO Slide-A-Lyzer Dialysis Cassette against 20 mM Tris. The refolded complex was purified using anion exchange and size exclusion HPLC and stored at –80°C in phosphate-buffered saline (PBS).

For some studies, biotinylation was carried out using an Avidity Biotinylation Kit (Avidity LLC), followed by HPLC purification.

UV-mediated peptide-exchange reactions.

UV-mediated peptide-exchange reactions were performed in either 0.6 mL conical tubes (Denville Scientific, C2170) or 96-well plates (CellTreat Scientific Products, 229190) to obtain pep/HLA complexes of interest. Each 115 μL reaction included 400 μM of exchange peptide and 4 μM of UV-peptide HLA-A2 monomer. Tubes or 96-well plates were placed in a CL-1000 Ultraviolet Crosslinker (AnalytikJena US LLC, Upland, CA) on ice for three, fifteen-minute increments. To maximize exchange efficiency, the samples were placed 5 cm from the UV lamp and mixed with a pipette between exposure intervals. After the reaction, each 115 μL sample was stored at 4°C in a 0.6 mL conical tube to avoid sample evaporation, which could potentially occur if peptides are stored in a plate. Reactions were stored for at least 48 hours prior to use in stability assays. For several complexes that have been tested after storage, we found that they were stable at 4°C for 10 months.

Flow cytometry-based half-life measurements.

A bead-based flow cytometry assay was used to measure pep/HLA-A2 dissociation rates with a soluble high-affinity TCR or with an antibody to β2m, as described previously (10). Biotinylated peptide/HLA-A2 complexes were coupled to streptavidin-coated microspheres (5 μm streptavidin-coated microspheres; Bangs Laboratories, Inc.) at a stoichiometry of about 2×10^7 complexes per microsphere. After incubation on ice for 30 minutes, the bead mixture was washed three times with PBS containing 1% bovine serum albumin (Gold Biotechnology, A-421–250), to remove unbound peptide/HLA-A2. Samples were then incubated at 37°C and aliquots were removed at various time points. Remaining (bound) peptide/HLA-A2 was determined by flow cytometry with an antibody to β2m (beta2-microglobulin mouse anti-human, clone B2M-01, PE conjugate; Invitrogen). In some experiments, a soluble, biotinylated high-affinity TCR to the WT-1/HLA-A2 complex, refolded and purified as previously described (18) (19), was used to compare the dissociation detected with anti-β2m. Mean fluorescence intensity was plotted against time for each point, and curves were fit with a first-order exponential decay curve to determine half-life value (OriginPro 2017, OriginLab, Northampton, MA). Each half-life value measured was the mean of two or more replicate experiments. Flow cytometry data obtained from an Accuri C6 (BD Biosciences, San Jose, CA) was analyzed with FCS Express 6 software to determine mean fluorescence values for each time point.

Differential scanning fluorimetry.

Differential scanning fluorimetry (DSF) was performed using a QuantStudio 7 Flex System real-time PCR machine (Applied Biosystems, Foster City, CA), 384-well Microamp optical plates (Applied Biosystems, 4309849), and Microamp adhesive film (Applied Biosystems, 4311971) for all peptide/HLA-A2 complexes. Each 20 μL reaction consisted of 2.5 μL of 40X SYPRO Orange® (Invitrogen) dye, 8.5 μL of molecular biology grade water, 5 μL of assay buffer (defined below), and the 4 μL of UV-exchanged complexes. SYPRO Orange® dye binds to hydrophobic regions of proteins that are exposed upon denaturation, resulting in fluorescence enhancement. DSF assay buffer consisted of 40 mM HEPES, 600 mM NaCl,

and 12 mM EDTA for most experiments at a pH of 7.4. We omitted the surfactant P20, used in a previous study (20). The real-time PCR machine was programmed for a temperature ramp rate of 1°C per minute from 25 to 99°C.

Determining T_m from non-linear fitting of thermal denaturation data.

Triplicate data points for each pep/HLA-A2 complex were analyzed using OriginPro 2017 software by plotting the fluorescence at each temperature measured (820 data points per reaction). Fluorescence data were processed and fit with a bi-Gaussian function to generate a curve with an R^2 value of 0.98 or greater. In some cases, it was necessary to truncate fluorescence values (by omitting early time points that exhibited no increase in fluorescence at low temperatures) in order to obtain a fit that accurately represented the data set. Complexes for which the bi-Gaussian fit resulted in an R^2 value lower than 0.98 were re-evaluated with an additional peptide exchange and DSF experiment. The first derivative of the curve obtained from bi-Gaussian fitting was used to calculate the precise midpoint (T_m).

Although the bi-Gaussian approach described above was used for all of the experiments reported here, we also compared two alternative approaches used previously to determine T_m values from fluorescence data. The first uses a Microsoft Excel macro called ‘deleteaftermax’ to automatically truncate datasets and remove post-peak quenching data (21). The sigmoidal denaturation curve was fit non-linearly to a Boltzmann Equation, and the T_m was obtained by finding the midpoint of the unfolding transition, or the peak of the first derivative curve. Comparison of DSF data analyzed with this method and the bi-Gaussian fit for various representative complexes showed similar results (Supplementary Table S1). A second approach determined the T_m by plotting the first derivative of the fluorescence emission as a function of temperature ($\partial F/\partial T$), processing the curve with the peak fitting algorithm in OriginPro 2017, applying a sigmoidal baseline, and fitting the peak of the derivative curve with a bi-Gaussian function (20). In our experience, this fitting technique requires high concentrations (10 μM and above) of pep/HLA complexes to achieve a high signal-to-noise ratio. The concentrations of complexes used were obtained by refolding each peptide with heavy chain and β2m, whereas the UV-exchange method used here yields lower concentrations of complexes but is required for high-throughput.

The Cancer Genome Atlas (TCGA) dataset analysis.—Gene expression and somatic mutation data of 266 skin cutaneous melanoma samples from TCGA, which were processed by Broad Institute’s TCGA workgroup (release date 10 October 2013), were downloaded and analyzed further (22,23). Briefly, 15,924 genes expressed in more than 80% of tumor samples were clustered using K-means clustering algorithm (k=12). Clusters containing 13 established T-cell signatures transcripts (CD8A, CCL2, CCL3, CCL4, CXCL9, CXCL10, ICOS, GZMK, IRF1, HLA-DMA, HLA-DMB, HLA-DOA, HLA-DOB) were selected to categorize 266 metastatic melanoma into T-cell gene signature high (called T-cell inflamed, or inflamed), T-cell gene signature intermediate, and T-cell gene signature low (called non-T-cell inflamed, or non-inflamed) tumor groups using ConsensusClusterPlus v.1.16.0 (24). Genes differentially expressed between T-cell inflamed and non-T-cell inflamed tumor groups were detected using ANOVA and filtered by false discovery rate. Synonymous single nucleotide variants were excluded from consideration. Data from patients predicted to be

HLA-A*0201-positive by two independent pipelines, ATHLATES (25) and PHLAT (26), were used to predict neoantigen peptide sequences with the Variant Effect Predictor v78 (27). Wild-type and altered 17-mer pairs were used to obtain 9-mer binding scores from the SYFPEITHI web server (28). In the present study, we selected 86 (Supplementary Table S7) and 91 (Supplementary Table S8) neoantigen peptides from the inflamed and non-inflamed tumor groups, respectively, for DSF analysis. Peptides were specifically chosen because they spanned a comparably large range (2 nM to 7,000 nM) of predicted binding affinities using NetMHC 4.0.

Statistical analysis.

For comparisons between the inflamed and non-inflamed TCGA cohort data, a two-tailed Student *t* test was used to determine significance, with significance accepted at $p < 0.05$. To compare T_m with half-life and binding affinity parameters, the x-axis was set to a logarithmic scale. R^2 values, based on the line of best fit, were determined using OriginPro 2017 software. T_m values and standard deviations reflect the average of a minimum of three replicates. Experimentally measured half-lives and standard deviations are the average of two independent time courses. Error bars for all figures indicate the standard deviation of replicates.

Results

Validation of differential scanning fluorimetry (DSF) as a high-throughput approach

A study has shown that DSF could be used with refolded and purified peptide/class I and / class II MHC complexes to measure thermal stability (20). In order for this approach to be high-throughput, it is necessary to develop a process that does not require individual refolding and purification of each complex. It is also important to demonstrate that thermal stability is directly correlated with half-life, as the latter appears to be correlated most closely with immunogenicity (10). To achieve these goals, we adapted the method of UV-cleavage of a modified peptide/HLA-A2 complex, in the presence of the peptide of interest, which yields peptide/HLA-A2 complexes (16), scaling down the typical reaction volume to increase the number of complexes that could be generated by a single preparation of UV peptide/HLA-A2. In initial studies, we examined thermal denaturation of complexes containing a peptide from Wilms tumor antigen (WT-1, RMFPNAPYL). Comparison of complexes using the UV-exchange procedure (Fig. 1A) or refolded and purified WT-1/HLA-A2 complexes (Fig. 1B) showed similar denaturation profiles and T_m values (see Materials and Methods for details) (Supplementary Fig S1). The UV peptide/HLA-A2 complex itself yielded a T_m value of 53.5°C (Fig. 1C). The replicates for these three complexes, conducted both in the same or different DSF experiments, was reproducible, with standard deviations of less than one degree (Supplementary Table S2).

To assess a range of T_m values, we next examined several additional peptides that are known to bind to HLA-A2 with different affinities and that are well studied. These complexes included the MART-1 nonomer (AAGIGILTV), MART-1 modified decamer (ELAGIGILTV), and tyrosinase (YMDGTMSQV) (Fig. 1D-F). We also included a number of other commonly studied self-peptides (Fig. 1G). T_m values of the complexes ranged from

43°C to 65°C, indicating that the method has a wide working range to compare stabilities. Reproducibility of the method was also evident by results with different UV-exchanged preparations for each of the three peptides, MART-1, WT-1, and tyrosinase (Fig. 1H). We have stored exchanged peptide complexes at 4°C for up to 10 months with identical DSF results to those from the initially tested complex.

Effects of DMSO, peptide purity, and pH on thermal denaturation

We examined the influence of three additional experimental parameters. First, peptides are often dissolved in DMSO in order to achieve greater solubility. To analyze the impact of DMSO, the UV-peptide/HLA-A2 complex was examined at various DMSO concentrations (Fig. 2A). Increasing concentrations of DMSO yielded a reduction in observed T_m values, such that there was approximately a 2°C difference between 1% and 10% DMSO. Our standard peptide exchange used a final DMSO concentration of 2% v/v and our DSF assay used a final DMSO concentration of 0.5% v/v.

In order to reduce the cost of commercial peptide synthesis, it is advantageous to use minimal purification (often called “crude” peptide scale from many sources). We compared a number of peptides that were ordered at the small-scale crude level versus the same peptides ordered with greater than 90% purity (Fig. 2B). The results showed nearly identical T_m values with each of the two preparations, suggesting that peptide purity levels for these 9-mer or 10-mer peptides did not significantly impact T_m values.

Finally, we noticed about a 3°C lower T_m value for the UV-peptide complex when DSF was run at a pH of 8.4 rather than 7.4. Analysis at a range of pH values showed that the temperature stability of complexes was reduced at an elevated pH (Fig. 2C). This same trend was observed for a larger collection of peptide complexes (Fig. 2D), indicating the need to analyze complexes at a consistent pH (from here on, we used pH7.4).

T_m and half-life comparisons of self-peptide variants

To determine if the temperature stability of UV-exchanged peptide/HLA-A2 complexes serves as a surrogate for half-lives, we used WT-1, MART-1, and their single-residue alanine variants. Because we have produced a high-affinity T-cell receptor (TCR) against WT-1/HLA-A2 (18), we used the soluble TCR as a probe for dissociation of the peptide from the ternary complex. This approach was compared with a similar experiment using anti-β2m as a probe for dissociation of β2m from the ternary complex, as has been used to determine half-lives of neoantigen HLA-A2 complexes (10). Biotinylated peptide/HLA-A2 complexes were immobilized on streptavidin-coated 5 μm microspheres, and the amount of complex that remained after dissociation at 37°C, at various time points, was determined by flow cytometry with anti-β2m or soluble TCR (Fig. 3A,B). Half-lives were determined by first-order kinetics of the dissociation curves, yielding values of 15.1hrs. and 14.7hrs., respectively. In order to examine a complex with a predicted shorter half-life, we also assessed the half-life of the anchor modified variant WT-1-M2A, which yielded half-lives of 1.2hrs. and 0.9hr with anti-β2m and TCR probes (Fig. 3C,D). These results support the view that the entire ternary complex dissociated with approximately the same kinetics.

We used DSF to determine the T_m values of WT-1 and MART-1 alanine variants (Fig. 4A,B, Supplementary Table S3). Reduced T_m values, compared to the wild-type peptide, would be expected for substitutions at anchor residues, such as the M2A substitution of WT-1. With M2A substitution, a 10°C lower T_m than the wild-type was observed, and other variants predicted to be at anchor residues also showed significantly lower T_m values (Fig. 4A). The structure of the WT-1 peptide within the WT-1/HLA-A2 complex (29) was shown to compare T_m values with the position of the side chains within the pocket of the class I molecule. Likewise, peptide variants of MART-1/HLA-A2 complexes were also analyzed for thermal stability, and T_m values are shown below the structure (30) of the MART-1 peptide (Fig. 4B). As expected, variants at anchor positions showed the largest reductions in T_m values. Changes from (or to) glycine often resulted in losses in stability, potentially due to conformational changes in backbone flexibility.

To directly compare the T_m values and half-lives of various complexes, we measured half-lives of complexes that spanned a roughly 20°C range of T_m values, using microspheres and anti-β2m (Supplementary Table S4). We found that the half-lives also spanned a wide range (0.6 to 82 hours) and that these two parameters were correlated (R^2=0.99; Fig. 4C).

T_m values correlate with reported half-lives of other HLA-A2 complexes

Buus and colleagues have measured the binding affinities and half-lives of various pep/HLA-A2 complexes and have found that for some peptides, the affinities for HLA-A2 do not correlate with half-life of the complex (9). To determine if T_m values correlated better with half-life or binding affinity, we synthesized a collection of peptides reported by Harndahl et al. (9), and used DSF to examine thermal stability of the UV-peptide exchanged complexes. The T_m values for these complexes correlated with their reported half-lives (R^2=0.94; Fig. 5A, Supplementary Table S5). In contrast, a plot of T_m values against measured binding affinity yielded a lower degree of correlation, whether using binding data from the approach of Assarson et al. (R^2 = 0.26) (31) or Harndahl et al. (R^2=0.60; Fig. 5B,C)(9). Two key peptides from the study in reference (9) that illustrated the distinction between affinity and half-life were the immunogenic peptide, FLTSVINRV and a non-immunogenic peptide, NQNDNEETV. These two peptide complexes had identical measured binding affinities, yet had half-lives of 22.3hrs. and 1.3hrs., respectively. These half-life values correlated with the T_m values of 58.0°C and 46.4°C for these two complexes, respectively. Thus, stability as measured by the dissociation of the complex correlated with thermal stability.

A study by Stronen et al. examined the half-lives of a collection of 57 neoantigen peptides derived from three melanoma patients, concluding that stability (half-lives) correlated better with immunogenicity (12 of the 57 peptides tested were judged to be immunogenic) than affinities predicted by the NetMHC4.0 algorithm (10). These 57 neoantigen peptides were synthesized and UV-peptide exchanged complexes were examined by DSF. A plot of T_m value versus half-life showed correlation (R^2=0.73; Fig. 5D, Supplementary Table S6). A lower correlation between T_m and half-life for this data set, relative to the correlations between T_m and half-life of the Harndahl et al. peptides (Fig. 5A) (9), may be attributed to those neoantigen complexes at the low end of the half-life range in the Stronen et al. study (10) (i.e. it appears that the assay did not resolve half-lives below values of about 3 hours). If

these values were eliminated, an R^2 value of 0.81 was observed (Fig. 5D). The previous study (10) suggested that neoantigen peptides with half-lives greater than 5 hours represent a reasonable 'cut-off' for choice of peptides with a higher probability of being immunogenic. The corresponding T_m value is about 53°C.

Correlation of T_m values with predicted binding affinities

Because prediction algorithms are often used as the sole approach to identify potential neoantigen peptides that bind to MHC, we compared the T_m data described above to predicted binding affinities using NetMHC4.0 (15). The plots for Harndahl et al. peptides (9), Stronen et al. peptides (10), and the WT-1/MART-1 variants and other self-peptides are shown in Fig. 5E-G. The R^2 values ranged from 0.38 to 0.62, lower than correlations with measured half-lives. The lower correlations observed between thermal stability and predicted affinity could be due to an actual difference in the two parameters (T_m and binding affinity, as suggested from data in Fig. 5B,C), the precision of the binding algorithm, or a combination of both.

T_m values of HLA-A2 complexes containing neoantigen peptides identified in TCGA

A study (22) analyzed whether there was a difference in the numbers and HLA-A2-binding quality of mutated peptides identified from WES analysis of 266 melanoma samples that exhibited either an inflamed or non-inflamed tumor microenvironment. The results suggested that no significant difference between the two sets of samples existed. In order to further examine these predicted neoantigens, we used DSF to analyze approximately 100 complexes from each inflamed or non-inflamed dataset, which had similar ranges of predicted HLA-A2 binding affinities (Fig. 6A,B). The measured T_m values of these two sets ranged from 35°C to 62°C, with distributions that were similar between the two sample types (Fig. 6C,D). The correlations of T_m values and predicted binding affinities (Fig. 6E,F) were similar to the correlations for peptides described above, providing further evidence that a DSF-based scan would allow improved identification of the most stable complexes. Statistical analysis using a two-tailed Student t-test (significance accepted at $p<0.05$) showed no significant differences between T_m measurements of inflamed and noninflamed tumor neoantigens ($p=0.39$). This observation further supports the view that neoantigen quantity or quality alone does not account for ability or inability to generate an inflamed tumor microenvironment.

T_m values of HLA-A2 complexes containing immunogenic neoantigen peptides

Several studies (12,32–36) have identified sequences of human neoantigen peptides that were found to elicit potent T-cell responses. From these studies, we had 26 peptides synthesized and examined them as HLA-A2 complexes using DSF. Although the T_m values ranged from 43 to 64°C (Table 1), 23 of the 26 complexes (88%) exhibited T_m values above 53°C, the temperature stability that we determined corresponded to a half-life of 5 hours, and 22/26 of the peptide complexes (85%) exhibited T_m values that were above 55°C. Thus, the majority of immunogenic peptides, derived from multiple published studies, exhibited high thermal stability as HLA-A2 complexes.

Discussion

Peptide-binding algorithms have been developed for many of the common HLA class I alleles (15,37,38). This has allowed for predictions of which mutated peptides identified in cancers could potentially bind to the HLA alleles expressed by a patient, with the goal of developing vaccine strategies to elicit T-cell responses against neoantigens expressed by cancer cells. In two vaccine trials in melanoma patients (12,13), the frequency of $CD8^+$ T-cell responses against these neoantigens was only 16% and 29%, respectively, indicating that improved methods for identifying immunogenic neoantigens are needed to improve patient responses. Because vaccine strategies require limits on the number of potential antigens (to date, between 10 and 20 peptides have been included), it is critical that those neoantigens with the highest probability of success be identified.

A number of studies have suggested that dissociation rates of peptide/HLA complexes are more accurate predictors of immunogenicity than binding affinity (e.g. (9,10)). Although some investigators have used the term ‘stability’ to refer to pepMHC dissociation rates, it should be noted that historically, stability studies of proteins use denaturants to quantitate the folded to unfolded transition. Accordingly, temperature or chaotropic agents (e.g. urea, guanidine) have been used to denature proteins or complexes, and stability is reflected in the temperature or the concentration of agent that yields 50% denaturation. These approaches also facilitate direct comparisons among different protein systems. Studies of pepMHC that examine dissociation rates are more accurately defined as a measure of ‘kinetic stability’, as has been done by some investigators (39).

Here, we took the more conventional biochemical approach using temperature denaturation to measure thermal stability of the pepMHC complexes. We demonstrated that 50% denaturation temperature (T_m) serves as a surrogate for dissociation rate. Our approach using UV-exchangeable reactions at small scale also facilitates high-throughput because thermal denaturation can be monitored rapidly using DSF in a standard RT-PCR thermal cycler. The DSF assay was validated using the HLA-A2 system, and a comprehensive collection of peptides from many previous studies. We also conducted our own analysis of dissociation rates using a panel of self-peptides that we have studied in the context of high-affinity T-cell receptor engineering (17,40).

HLA-A2 complexes exhibited T_m values with a working range of over 20°C and standard deviations that were generally less than 0.5°C, even when complexes were prepared from different UV-exchange reactions. The T_m values using five complexes derived from the UV-exchange procedure (MART-1–9mer, WT1, MART1–10mer, TAX, Tyrosinase: 43.7°C, 57.8°C, 59.3°C, 61.9°C, 65.5°C) were very similar to the T_m values determined by another lab where each complex was refolded with HLA-A2 individually (40.8°C, 56.3°C, 59.4°C, 66.3°C, 67.3°C, respectively)(R^2 value 0.97)(20). This indicated that the DSF approach is not only amenable to high-throughput UV-exchange but that results are comparable among different labs.

T_m values correlated with half-lives measured for a panel of self-peptides and single amino acid variants (R^2=0.99). As expected, lower T_m values were observed for peptides with

substitutions at anchor residues. We also noted that peptides with substitutions to or from glycine, even in non-anchor residues, often yielded altered T_m values. The binding affinities of glycine-substituted peptides were predicted less accurately than most other substitutions by NetMHC4.0. The ability of glycine residues to influence backbone conformations, and the impact on adjacent residues, likely accounts for these observations. This result also further illustrated the value of conducting experimental stability assessments, rather than relying only on predictive algorithms.

Analysis of a collection of peptides, comprising other self-peptides and neoantigens, for which published half-lives were determined by independent methods also showed correlation with T_m values. As experimentally measured binding affinities were available for some of these peptides, we were able to show that thermal stability correlated more closely with dissociation rate than with affinity. A study analyzing peptides from the human tumor antigen NY-ESO-1 also showed weak correlation between half-life and either measured or predicted binding affinity (41).

These findings raise the mechanistic question of why thermal stability is correlated with kinetic stability, whereas either stability parameter has a lower correlation with measured or predicted binding affinity. The likely explanation for the high correlation between thermal and kinetic stability is that each measurement is performed with the ternary pepMHC complex and the same atomic interactions that control dissociation of the complex control its temperature denaturation. In contrast, binding affinities involve both association and dissociation rates of the complexes. Measurements of peptide affinities for MHC heavy chain/β2m are not trivial (42) and involve competition assays with labeled indicator peptides as pioneered by Sette et al. (43), refolding reactions (44), or surface plasmon resonance (45). In any case, association rates of peptides are expected to impact the final measurement, and these association rates likely vary among peptides. This possibility is supported by evidence that dynamics of the MHC molecule or the peptide influence the interaction (46). The conformational effects of such dynamics could impact the association rates. Hence, it is not surprising that the stability of the ternary complex (which is not influenced by association rate) does not always correlate with affinity. Peptide binding affinity methods are inherently complicated (42), as the MHC heavy chain/β2m dimer is not stable without a peptide, preventing direct binding studies. These assays are also sensitive to other conditions of the assay, as we have shown here with the impact of pH on thermal stability.

The lower correlation between stability and predicted affinity could be influenced by the same issues as measured affinity (e.g. association rate contributes to affinity). However, an algorithm based on stability data has also been developed (NetMHCStab, (47)), and this also showed a low correlation when the T_m values measured here were plotted versus the predicted stability (R^2 value=0.49). The most likely explanation for this is that prediction algorithms (affinity or stability) have insufficient training sets to encompass all sequence space. The thermal stability results with the glycine-substituted peptides in our study illustrates an example of this problem. Although future algorithms might improve these predictions, experimental measures of stability, such as the DSF method described here, are needed to analyze peptide/MHC complexes.

The residence time (48) of the ternary pepMHC complex on the cell surface is important physiologically because specific T cells must have sufficient time to survey and interact with the target cells. Such T cells are sensitive to the density of the antigenic complex (49). Antigen processing steps preceding surface expression of the complex are also critical (50). The ability to elicit tumor-reactive cytotoxic T lymphocytes requires not only that the peptide be bound by a class I molecule but that the protein is translated and processed in sufficient quantities. Potential neoantigen peptides with high stability as a complex might not be expressed on the surface because the peptide processing machinery might be unable to cleave or deliver the peptide efficiently or assemble the final complex (50). Strategies to quantify these steps for each peptide would be valuable but are difficult to examine in a high-throughput format. The rules that govern whether a peptide is processed and presented are topics of interest, but improvements in mass spectrometry methods to detect and quantitate peptides eluted from MHC should provide additional insight (51–53). Finally, for a peptide to be immunogenic, antigen-reactive T cells must exist in the repertoire to respond to the complex.

It has been suggested that immunogenicity often involves TCR-mediated interactions with central residues of a peptide (e.g. positions 4 and 5), and that hydrophobic side chains increase the chance of immunogenicity (54,55). Studies have developed an immunogenicity ‘fitness’ algorithm based on the similarity of peptides to a library of known immunogenic foreign peptides (56). Immunogenicity can also be influenced by the degree of tolerance against self or mutated peptides, and we have argued that tolerance may be controlled by the size of the repertoire of structurally related self-peptides (57). Once these factors are more fully understood, it should be possible to develop algorithms that improve the success rate of neoantigen-based vaccines.

In summary, the DSF assay will allow high-throughput experimental identification of the most stable neoantigen peptides, derived from WES/RNA-sequence data, at a scale required for treatment of larger patient populations. For example, on a research level scale, the amount of refolded UV-peptide/HLA-A2 protein is sufficient for performing DSF with thousands of peptides, and the 384-well format used in most RT-PCR machines will allow robotic assay development. Production of many different class I alleles will enable direct comparisons of T_m values across alleles, a feature that can accommodate variation in predictive accuracy of binding algorithms among alleles.

Supplementary Material

Refer to Web version on PubMed Central for supplementary material.

Acknowledgements

We thank Abby Brown for experimental assistance and Brian Baker and Lance Hellman (University of Notre Dame) for helpful discussions about DSF analysis. We thank Barbara Pilas and the Roy J. Carver Biotechnology Center (CBC) Flow Cytometry Facility and Mark Band of the Functional Genomics Unit for the use of their real-time PCR equipment.

Financial support: This work was supported by National Institutes of Health grants CA178844 and CA187592 (to D.M.K.)

Abbreviations

The abbreviations used are:

DSF	Differential Scanning Fluorimetry
TCR	T Cell Receptor
pepMHC	peptide complexed with major histocompatibility complex
HLA	human leukocyte antigen (refers to human major histocompatibility complex alleles)
Tm	melting temperature
UV	ultraviolet

References

1. Gubin MM, Zhang X, Schuster H, Caron E, Ward JP, Noguchi T, et al. Checkpoint blockade cancer immunotherapy targets tumour-specific mutant antigens. Nature 2014;515(7528):577–81 doi 10.1038/nature13988. [PubMed: 25428507]
2. Ribas A, Wolchok JD. Cancer immunotherapy using checkpoint blockade. Science 2018;359(6382): 1350–5 doi 10.1126/science.aar4060. [PubMed: 29567705]
3. Schumacher TN, Schreiber RD. Neoantigens in cancer immunotherapy. Science 2015;348(6230): 69–74 doi 10.1126/science.aaa4971. [PubMed: 25838375]
4. Blank CU, Haanen JB, Ribas A, Schumacher TN. CANCER IMMUNOLOGY. The “cancer immunogram”. Science 2016;352(6286):658–60 doi 10.1126/science.aaf2834. [PubMed: 27151852]
5. Schumacher TN, Hacohen N. Neoantigens encoded in the cancer genome. Curr Opin Immunol 2016;41:98–103 doi 10.1016/j.coi.2016.07.005. [PubMed: 27518850]
6. Tran E, Robbins PF, Rosenberg SA. ‘Final common pathway’ of human cancer immunotherapy: targeting random somatic mutations. Nature immunology 2017;18(3):255–62 doi 10.1038/ni.3682. [PubMed: 28198830]
7. Hu Z, Ott PA, Wu CJ. Towards personalized, tumour-specific, therapeutic vaccines for cancer. Nature reviews Immunology 2018;18(3):168–82 doi 10.1038/nri.2017.131.
8. Sahin U, Tureci O. Personalized vaccines for cancer immunotherapy. Science 2018;359(6382): 1355–60 doi 10.1126/science.aar7112. [PubMed: 29567706]
9. Harndahl M, Rasmussen M, Roder G, Dalgaard Pedersen I, Sorensen M, Nielsen M, et al. Peptide-MHC class I stability is a better predictor than peptide affinity of CTL immunogenicity. Eur J Immunol 2012;42(6):1405–16 doi 10.1002/eji.201141774. [PubMed: 22678897]
10. Stronen E, Toebes M, Kelderman S, van Buuren MM, Yang W, van Rooij N, et al. Targeting of cancer neoantigens with donor-derived T cell receptor repertoires. Science 2016;352(6291):1337–41 doi 10.1126/science.aaf2288. [PubMed: 27198675]
11. Editorial. The problem with neoantigen prediction. Nature biotechnology 2017;35(2):97 doi 10.1038/nbt.3800.
12. Ott PA, Hu Z, Keskin DB, Shukla SA, Sun J, Bozym DJ, et al. An immunogenic personal neoantigen vaccine for patients with melanoma. Nature 2017;547(7662):217–21 doi 10.1038/nature22991. [PubMed: 28678778]
13. Sahin U, Derhovanessian E, Miller M, Kloke BP, Simon P, Lower M, et al. Personalized RNA mutanome vaccines mobilize poly-specific therapeutic immunity against cancer. Nature 2017;547(7662):222–6 doi 10.1038/nature23003. [PubMed: 28678784]
14. Niesen FH, Berglund H, Vedadi M. The use of differential scanning fluorimetry to detect ligand interactions that promote protein stability. Nat Protoc 2007;2(9):2212–21 doi 10.1038/nprot.2007.321. [PubMed: 17853878]

15. Andreatta M, Nielsen M. Gapped sequence alignment using artificial neural networks: application to the MHC class I system. Bioinformatics (Oxford, England) 2016;32(4):511–7 doi 10.1093/bioinformatics/btv639.

16. Rodenko B, Toebes M, Hadrup SR, van Esch WJ, Molenaar AM, Schumacher TN, et al. Generation of peptide-MHC class I complexes through UV-mediated ligand exchange. Nat Protoc 2006;1(3):1120–32 doi nprot.2006.121 [pii]10.1038/nprot.2006.121. [PubMed: 17406393]

17. Sharma P, Kranz DM. Subtle changes at the variable domain interface of the T-cell receptor can strongly increase affinity. J Biol Chem 2018;293(5):1820–34 doi 10.1074/jbc.M117.814152. [PubMed: 29229779]

18. Harris DT, Hager MV, Smith SN, Cai Q, Stone JD, Kruger P, et al. Comparison of T Cell Activities Mediated by Human TCRs and CARs That Use the Same Recognition Domains. J Immunol 2018;200(3):1088–100 doi 10.4049/jimmunol.1700236. [PubMed: 29288199]

19. Zhang B, Bowerman NA, Salama JK, Schmidt H, Spiotto MT, Schietinger A, et al. Induced sensitization of tumor stroma leads to eradication of established cancer by T cells. J Exp Med 2007;204(1):49–55. [PubMed: 17210731]

20. Hellman LM, Yin L, Wang Y, Blevins SJ, Riley TP, Belden OS, et al. Differential scanning fluorimetry based assessments of the thermal and kinetic stability of peptide-MHC complexes. Journal of immunological methods 2016;432:95–101 doi 10.1016/j.jim.2016.02.016. [PubMed: 26906089]

21. Huynh K, Partch CL. Analysis of protein stability and ligand interactions by thermal shift assay. Current protocols in protein science 2015;79:28.9.1–14 doi 10.1002/0471140864.ps2809s79. [PubMed: 25640896]

22. Spranger S, Luke JJ, Bao R, Zha Y, Hernandez KM, Li Y, et al. Density of immunogenic antigens does not explain the presence or absence of the T-cell-inflamed tumor microenvironment in melanoma. Proc Natl Acad Sci U S A 2016;113(48):E7759–e68 doi 10.1073/pnas.1609376113. [PubMed: 27837020]

23. Spranger S, Bao R, Gajewski TF. Melanoma-intrinsic beta-catenin signalling prevents anti-tumour immunity. Nature 2015;523(7559):231–5 doi 10.1038/nature14404. [PubMed: 25970248]

24. Wilkerson MD, Hayes DN. ConsensusClusterPlus: a class discovery tool with confidence assessments and item tracking. Bioinformatics (Oxford, England) 2010;26(12):1572–3 doi 10.1093/bioinformatics/btq170.

25. Liu C, Yang X, Duffy B, Mohanakumar T, Mitra RD, Zody MC, et al. ATHLATES: accurate typing of human leukocyte antigen through exome sequencing. Nucleic acids research 2013;41(14):e142 doi 10.1093/nar/gkt481. [PubMed: 23748956]

26. Bai Y, Ni M, Cooper B, Wei Y, Fury W. Inference of high resolution HLA types using genome-wide RNA or DNA sequencing reads. BMC genomics 2014;15:325 doi 10.1186/1471-2164-15-325. [PubMed: 24884790]

27. McLaren W, Pritchard B, Rios D, Chen Y, Flicek P, Cunningham F. Deriving the consequences of genomic variants with the Ensembl API and SNP Effect Predictor. Bioinformatics (Oxford, England) 2010;26(16):2069–70 doi 10.1093/bioinformatics/btq330.

28. Rammensee H, Bachmann J, Emmerich NP, Bachor OA, Stevanovic S. SYFPEITHI: database for MHC ligands and peptide motifs. Immunogenetics 1999;50(3–4):213–9. [PubMed: 10602881]

29. Borbulevych OY, Do P, Baker BM. Structures of native and affinity-enhanced WT1 epitopes bound to HLA-A*0201: implications for WT1-based cancer therapeutics. Molecular immunology 2010;47(15):2519–24 doi S0161–5890(10)00474–8 [pii]10.1016/j.molimm.2010.06.005. [PubMed: 20619457]

30. Sliz P, Michielin O, Cerottini JC, Luescher I, Romero P, Karplus M, et al. Crystal structures of two closely related but antigenically distinct HLA-A2/melanocyte-melanoma tumor-antigen peptide complexes. J Immunol 2001;167(6):3276–84. [PubMed: 11544315]

31. Assarsson E, Sidney J, Oseroff C, Pasquetto V, Bui HH, Frahm N, et al. A quantitative analysis of the variables affecting the repertoire of T cell specificities recognized after vaccinia virus infection. J Immunol 2007;178(12):7890–901. [PubMed: 17548627]

32. Fritsch EF, Rajasagi M, Ott PA, Brusic V, Hacohen N, Wu CJ. HLA-binding properties of tumor neoepitopes in humans. Cancer immunology research 2014;2(6):522–9 doi 10.1158/2326-6066.cir-13-0227. [PubMed: 24894089]
33. Robbins PF, Lu YC, El-Gamil M, Li YF, Gross C, Gartner J, et al. Mining exomic sequencing data to identify mutated antigens recognized by adoptively transferred tumor-reactive T cells. Nat Med 2013;19(6):747–52 doi nm.3161 [pii]10.1038/nm.3161. [PubMed: 23644516]
34. Cohen CJ, Gartner JJ, Horovitz-Fried M, Shamalov K, Trebska-McGowan K, Bliskovsky VV, et al. Isolation of neoantigen-specific T cells from tumor and peripheral lymphocytes. J Clin Invest 2015;125(10):3981–91 doi 10.1172/jci82416. [PubMed: 26389673]
35. Prickett TD, Crystal JS, Cohen CJ, Pasetto A, Parkhurst MR, Gartner JJ, et al. Durable Complete Response from Metastatic Melanoma after Transfer of Autologous T Cells Recognizing 10 Mutated Tumor Antigens. Cancer immunology research 2016;4(8):669–78 doi 10.1158/2326-6066.cir-15-0215. [PubMed: 27312342]
36. Durgeau A, Virk Y, Corgnac S, Mami-Chouaib F. Recent Advances in Targeting CD8 T-Cell Immunity for More Effective Cancer Immunotherapy. Front Immunol 2018;9:14 doi 10.3389/fimmu.2018.00014. [PubMed: 29403496]
37. Jurtz V, Paul S, Andreatta M, Marcatili P, Peters B, Nielsen M. NetMHCpan-4.0: Improved Peptide-MHC Class I Interaction Predictions Integrating Eluted Ligand and Peptide Binding Affinity Data. J Immunol 2017;199(9):3360–8 doi 10.4049/jimmunol.1700893. [PubMed: 28978689]
38. Rasmussen M, Fenoy E, Harndahl M, Kristensen AB, Nielsen IK, Nielsen M, et al. Pan-Specific Prediction of Peptide-MHC Class I Complex Stability, a Correlate of T Cell Immunogenicity. J Immunol 2016;197(4):1517–24 doi 10.4049/jimmunol.1600582. [PubMed: 27402703]
39. Lazarski CA, Chaves FA, Jenks SA, Wu S, Richards KA, Weaver JM, et al. The kinetic stability of MHC class II:peptide complexes is a key parameter that dictates immunodominance. Immunity 2005;23(1):29–40 doi 10.1016/j.immuni.2005.05.009. [PubMed: 16039577]
40. Smith SN, Sommermeyer D, Piepenbrink KH, Blevins SJ, Bernhard H, Uckert W, et al. Plasticity in the Contribution of T Cell Receptor Variable Region Residues to Binding of Peptide-HLA-A2 Complexes. J Mol Biol 2013;425(22):4496–507 doi S0022–2836(13)00510-X [pii]10.1016/j.jmb.2013.08.007. [PubMed: 23954306]
41. Schmidt J, Guillaume P, Dojcinovic D, Karbach J, Coukos G, Luescher I. In silico and cell-based analyses reveal strong divergence between prediction and observation of T-cell-recognized tumor antigen T-cell epitopes. J Biol Chem 2017;292(28):11840–9 doi 10.1074/jbc.M117.789511. [PubMed: 28536262]
42. Margulies DH, Corr M, Boyd LF, Khilko SN. MHC class I/peptide interactions: binding specificity and kinetics. Journal of molecular recognition : JMR 1993;6(2):59–69 doi 10.1002/jmr.300060204. [PubMed: 8305252]
43. Sidney J, Southwood S, Moore C, Oseroff C, Pinilla C, Grey HM, et al. Measurement of MHC/peptide interactions by gel filtration or monoclonal antibody capture. Current protocols in immunology 2013;Chapter 18:Unit 18.3. doi 10.1002/0471142735.im1803s100.
44. Harndahl M, Justesen S, Lamberth K, Roder G, Nielsen M, Buus S. Peptide binding to HLA class I molecules: homogenous, high-throughput screening, and affinity assays. Journal of biomolecular screening 2009;14(2):173–80 doi 10.1177/1087057108329453. [PubMed: 19196700]
45. Khilko SN, Corr M, Boyd LF, Lees A, Inman JK, Margulies DH. Direct detection of major histocompatibility complex class I binding to antigenic peptides using surface plasmon resonance. Peptide immobilization and characterization of binding specificity. J Biol Chem 1993;268(21):15425–34. [PubMed: 8393442]
46. Ayres CM, Corcelli SA, Baker BM. Peptide and Peptide-Dependent Motions in MHC Proteins: Immunological Implications and Biophysical Underpinnings. Front Immunol 2017;8:935 doi 10.3389/fimmu.2017.00935. [PubMed: 28824655]
47. Jorgensen KW, Rasmussen M, Buus S, Nielsen M. NetMHCstab - predicting stability of peptide-MHC-I complexes; impacts for cytotoxic T lymphocyte epitope discovery. Immunology 2014;141(1):18–26 doi 10.1111/imm.12160. [PubMed: 23927693]

48. Tummino PJ, Copeland RA. Residence time of receptor-ligand complexes and its effect on biological function. Biochemistry 2008;47(20):5481–92 doi 10.1021/bi8002023. [PubMed: 18412369]

49. Chervin AS, Stone JD, Holler PD, Bai A, Chen J, Eisen HN, et al. The impact of TCR-binding properties and antigen presentation format on T cell responsiveness. J Immunol 2009;183(2): 1166–78 doi jimmunol.0900054 [pii]10.4049/jimmunol.0900054. [PubMed: 19553539]

50. Blum JS, Wearsch PA, Cresswell P. Pathways of antigen processing. Annu Rev Immunol 2013;31:443–73 doi 10.1146/annurev-immunol-032712-095910. [PubMed: 23298205]

51. Bassani-Sternberg M, Coukos G. Mass spectrometry-based antigen discovery for cancer immunotherapy. Curr Opin Immunol 2016;41:9–17 doi 10.1016/j.coi.2016.04.005. [PubMed: 27155075]

52. Muller M, Gfeller D, Coukos G, Bassani-Sternberg M. 'Hotspots' of Antigen Presentation Revealed by Human Leukocyte Antigen Ligandomics for Neoantigen Prioritization. Front Immunol 2017;8:1367 doi 10.3389/fimmu.2017.01367. [PubMed: 29104575]

53. Creech AL, Ting YS, Goulding SP, Sauld JFK, Barthelme D, Rooney MS, et al. The Role of Mass Spectrometry and Proteogenomics in the Advancement of HLA Epitope Prediction. Proteomics 2018 doi 10.1002/pmic.201700259.

54. Calis JJ, Maybeno M, Greenbaum JA, Weiskopf D, De Silva AD, Sette A, et al. Properties of MHC class I presented peptides that enhance immunogenicity. PLoS Comput Biol 2013;9(10):e1003266 doi 10.1371/journal.pcbi.1003266. [PubMed: 24204222]

55. Chowell D, Krishna S, Becker PD, Cocita C, Shu J, Tan X, et al. TCR contact residue hydrophobicity is a hallmark of immunogenic CD8+ T cell epitopes. Proc Natl Acad Sci U S A 2015;112(14):E1754–62 doi 10.1073/pnas.1500973112. [PubMed: 25831525]

56. Luksza M, Riaz N, Makarov V, Balachandran VP, Hellmann MD, Solovyov A, et al. A neoantigen fitness model predicts tumour response to checkpoint blockade immunotherapy. Nature 2017;551(7681):517–20 doi 10.1038/nature24473. [PubMed: 29132144]

57. Stone JD, Harris DT, Kranz DM. TCR affinity for p/MHC formed by tumor antigens that are self-proteins: impact on efficacy and toxicity. Curr Opin Immunol 2015;33:16–22 doi 10.1016/j.coi.2015.01.003. [PubMed: 25618219]

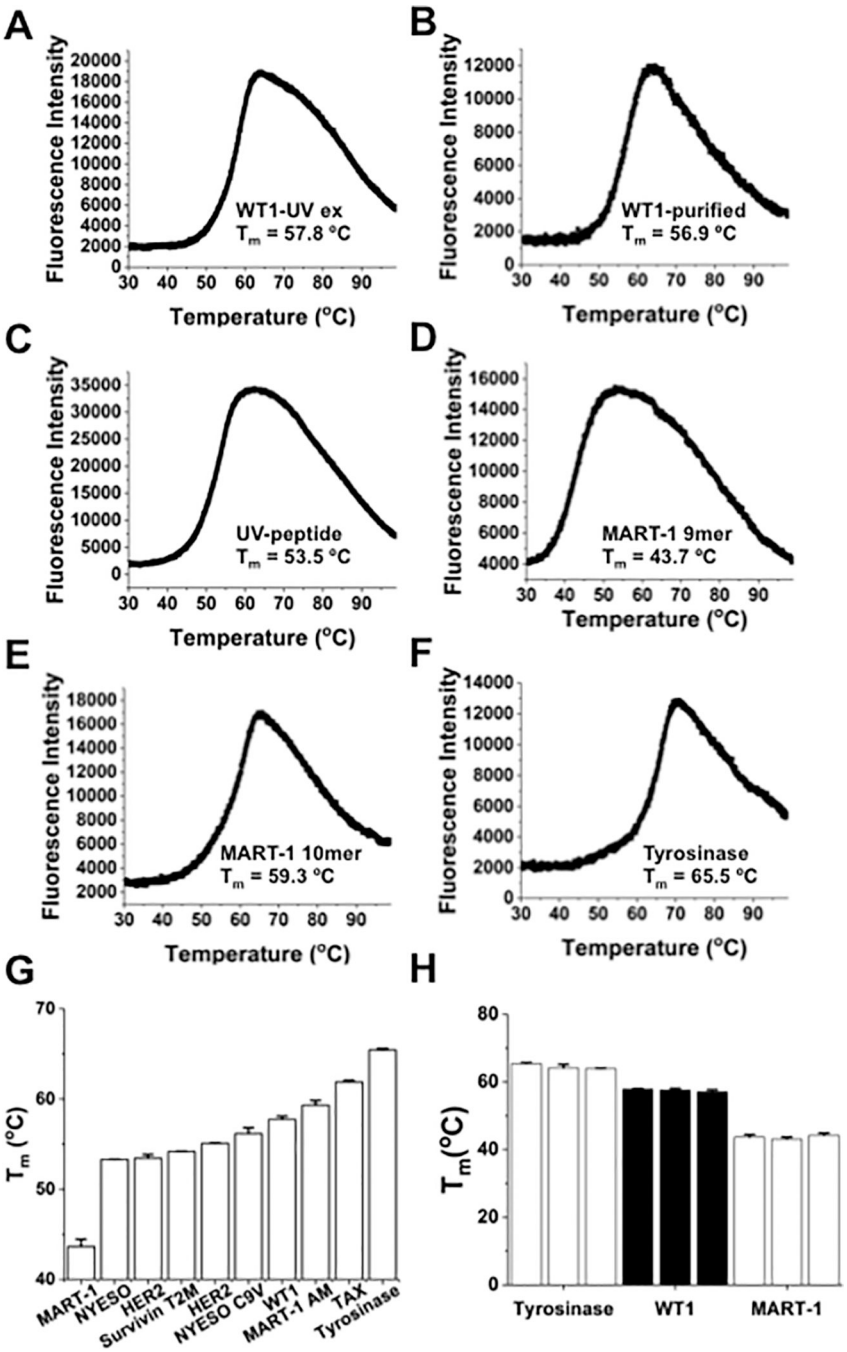

Figure 1. Thermal denaturation curves generated from differential scanning fluorimetry (DSF) of self-peptide/HLA-A2 complexes.

(A) DSF denaturation profile of WT-1 (RMFPNAPYL)/HLA-A2 complex prepared through UV-mediated ligand exchange at 4 uM. For all measurements, the temperature ramp rate was 1°C/minute from 25°C to 99°C. The curve was created using OriginPro 2017 software to plot all 820 time points generated from QuantStudio™ Real-Time PCR. **(B)** Thermal denaturation curve of refolded WT-1/HLA-A2 monomer at 4 uM, used for comparison with UV-generated complex. **(C)** DSF profile of refolded UV-peptide/HLA-A2. The UV-peptide

(KILGFVFJV) contains 3-amino-3-(2-nitro)phenyl-propionic acid, denoted with a J in the peptide sequence. **(D-F)** DSF profiles for UV-exchanged self-peptide/HLA-A2 complexes with MART-1 9-mer (AAGIGILTV), MART-1 anchor-modified 10-mer (ELAGIGILTV), and Tyrosinase (YMDGTMSQV). For **(A-F)**, curves are representative of 3 independent experiments, with three replicates per experiment. **(G)** Comparison of T_m values from several well-characterized self-peptides, including NYESO-1 (SLLMWITNC) and HER2 (KIFGSLAFL). **(H)** Comparison of T_m values from three separate DSF experiments with UV-exchanged self-peptide/HLA-A2 complexes. UV-exchanged complexes with Tyrosinase (YMDGTMSQV), WT-1 (RMFPNAPYL), and MART-1 (AAGIGILTV) were analyzed in three separate experiments of three replicates each. Different UV-exchanged preparations were used for each trial. Error bars represent the standard deviation between replicates of individual DSF runs.

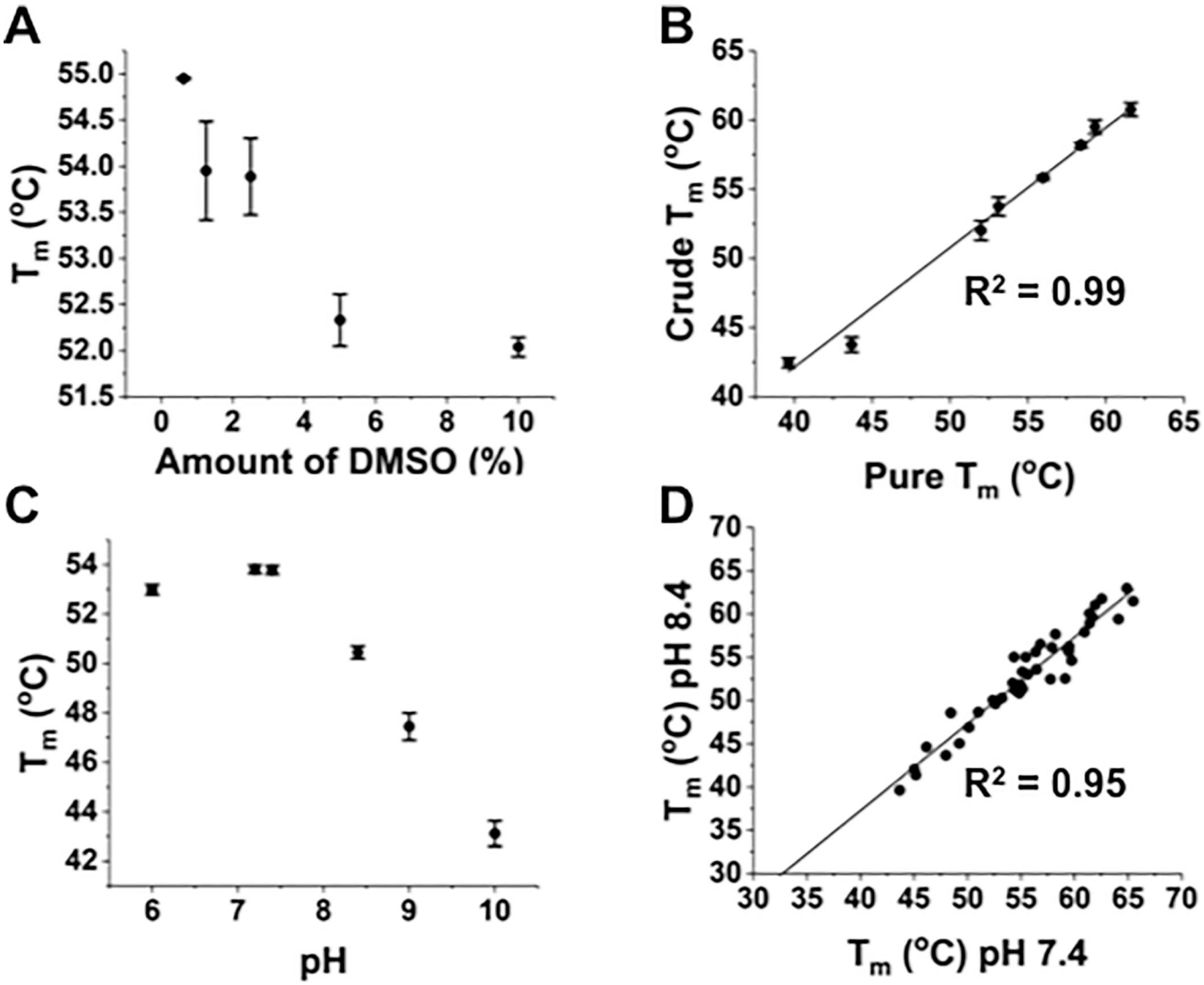

Figure 2. Effects of DMSO, peptide purity, and pH on thermal denaturation of pep/HLA-A2 complexes.

(A) T_m values of UV-peptide/HLA-A2 in PBS and various concentrations of dimethyl sulfoxide (DMSO). The UV-exchange method uses peptides dissolved in DMSO, yielding final concentrations of DMSO present at 0.5% in a typical DSF experiment. **(B)** Comparison of T_m values from DSF of HLA-A2 complexes generated with either pure (90%) or crude (as low as 30%) peptide preparations. Correlation co-efficient (R^2=0.99) was calculated using OriginPro 2017. **(C)** T_m values were determined by DSF at various pH values, using assay buffers containing HEPES, boric acid, or acetic acid. Unless otherwise noted, all subsequent DSF experiments were performed at pH 7.4 using HEPES as the assay buffer. **(D)** Comparison of T_m values (R^2 = 0.95) from various self-peptide/HLA-A2 and neoantigen/HLA-A2 complexes at pH 7.4 and pH 8.4. Melting temperatures were increased at 7.4 (compared to pH 8.4) by an average of 2.5°C. Error bars represent the average and standard deviation of three replicates in a single experiment.

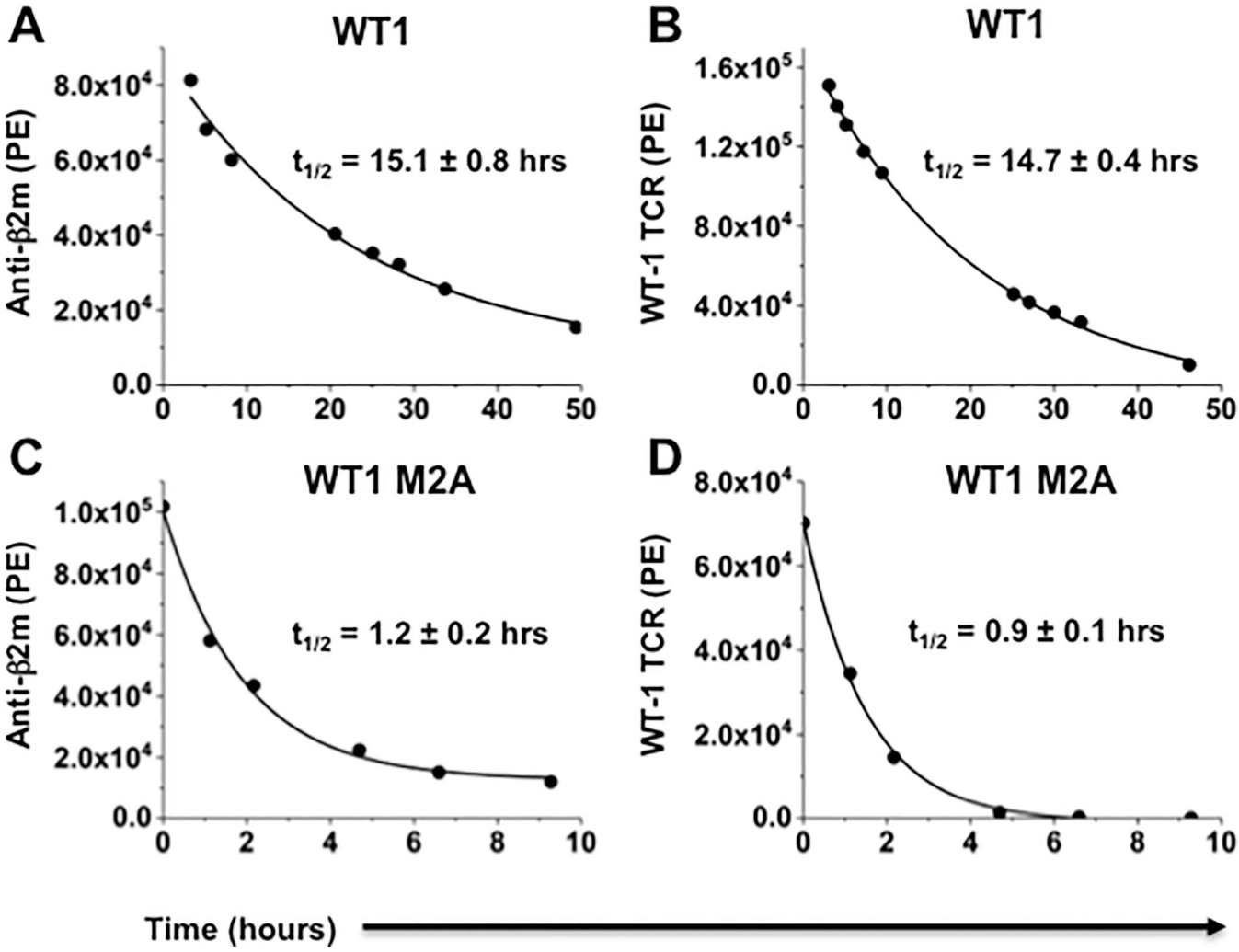

Figure 3. Dissociation measurements of WT-1/HLA-A2 complexes using two different probes.

(A) Dissociation curve of WT-1/HLA-A2 complexes using anti-β2m as a probe ($t_{1/2}$=15.7). **(B)** Dissociation curve of WT-1/HLA-A2 complexes using soluble high-affinity T-cell receptor (TCR) as a probe ($t_{1/2}$ =14.4). **(C)** Dissociation curve of WT-1–M2A complexes, a reduced stability variant (RAFPNAPYL), using anti-β2m ($t_{1/2}$=1.3). **(D)** Dissociation curve of WT-1–M2A/HLA-A2 using soluble TCR ($t_{1/2}$=1.0). In these experiments, refolded WT-1/HLA-A2 or WT-1–M2A/HLA-A2 were biotinylated with BirA ligase, purified by HPLC ion exchange and gel filtration chromatography, and immobilized on SA-coated 5 μm microspheres. Curves show data from a single experiment, representative of two independent experiments, with one replicate each. Half-life values are the averages of two independent experiments, with one replicate each.

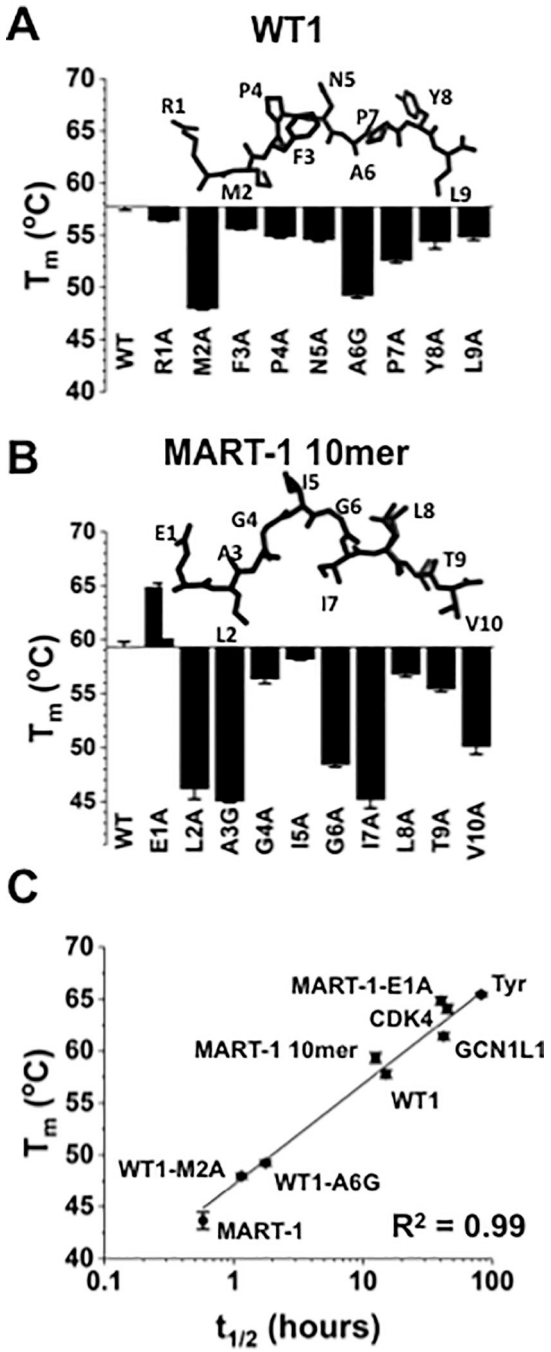

Figure 4. DSF analysis of self-peptides and single peptide variants.

(A) Comparison of T_m values for self-peptide WT-1 (RMFPNAPYL) and its alanine variants. In positions where an alanine was present in the wild-type sequence, it was replaced with a glycine (WT1-A6G). The structure of the WT-1 peptide from the WT-1/HLA-A2 structure is shown (PDB: 3HPJ). **(B)** T_m values for MART-1 anchor-modified 10-mer (ELAGIGILTV) and its alanine variants. In positions where an alanine was present in the wild-type sequence, it was replaced with a glycine (MART1-A3G). The structure of the MART-1 10mer peptide from the MART-1/HLA-A2 structure is shown (PDB: 1JF1). **(C)**

Correlation (R^2=0.99) between half-lives measured experimentally using the anti-β2m probe and T_m values obtained from DSF. Error bars represent the average and standard deviation of two independent experiments, with three replicates per experiment.

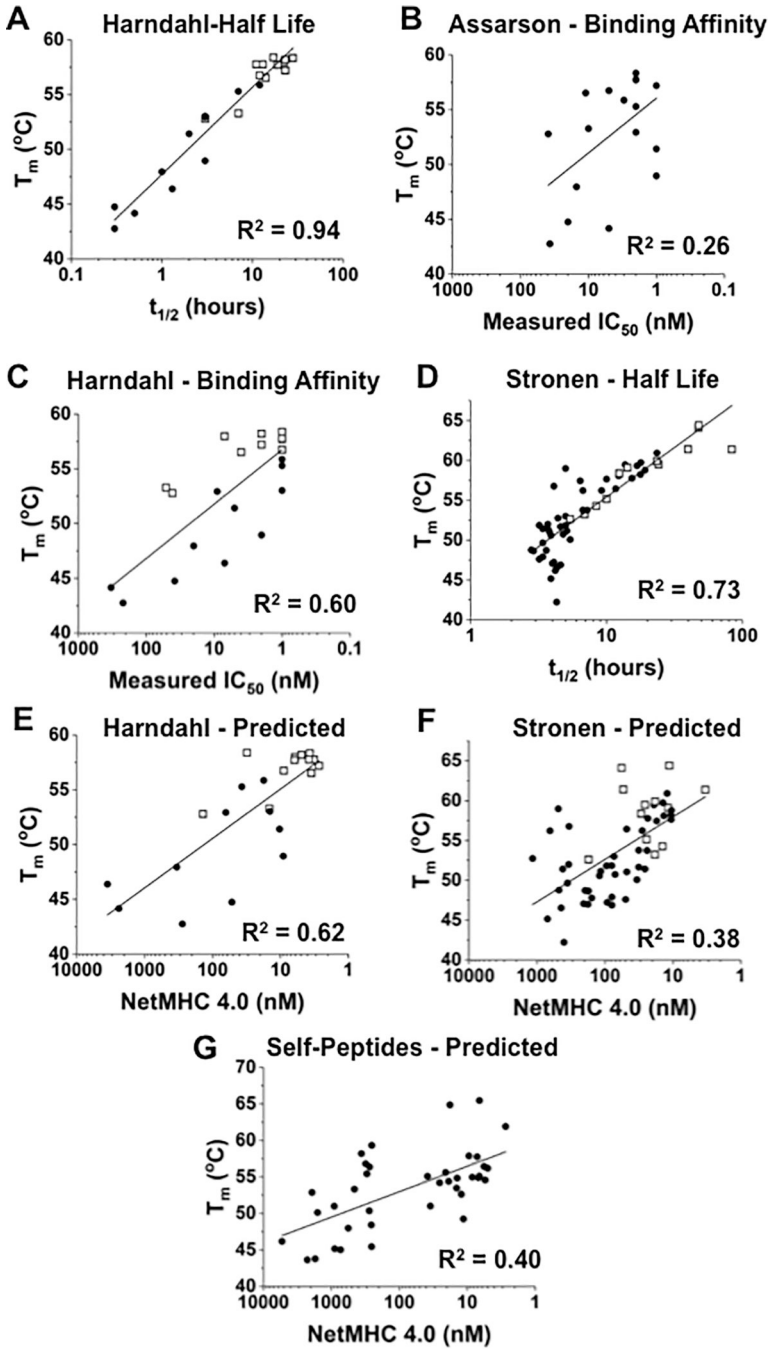

Figure 5. Correlation of T_m values with half-lives, predicted binding affinities, or measured binding affinities.

(A) Plot of T_m values, determined by DSF, versus half-lives for 23 T-cell epitopes restricted by HLA-A2 (9). Epitopes reported as immunogenic are shown in open squares (R^2=0.94). **(B, C)** Peptides with known binding affinity measurements analyzed by Assarson et al. (31) and Harndahl et al. (9) were examined by DSF and T_m values were plotted versus IC_{50} measurements from Assarson et al. (R^2=0.26) or Harndahl et al. (R^2=0.60). Epitopes that they defined as immunogenic are shown in open squares. **(D)** Plot of T_m values, determined

by DSF, versus half-lives of 53 HLA-A2 restricted neoantigens derived from three melanoma patients (10). The correlation (R^2=0.73) between published half-lives and measured T_m values was increased (R^2=0.81) if data for those peptides that reached the shortest measurable half-life (10). Immunogenic neoantigens (12 of 53) from the latter study are shown in open squares. **(E)** Correlation (R^2=0.62) between binding affinity, predicted *in silico* with NetMHC 4.0, and experimentally measured T_m values for the 23 unique T-cell epitopes (9). Immunogenic epitopes are shown in open squares. **(F)** Correlation (R^2=0.39) between binding affinity, predicted *in silico* with NetMHC 4.0, and experimentally measured T_m values for 53 melanoma-specific, HLA-A2–restricted neoantigens (10). The 12 immunogenic neoantigens are shown in open squares. **(G)** Correlation (R^2=0.40) between binding affinity, predicted *in silico* with NetMHC 4.0, and experimentally measured T_m values for HLA-A2–restricted self-peptides or their single peptide variants (Supplementary Table S2).

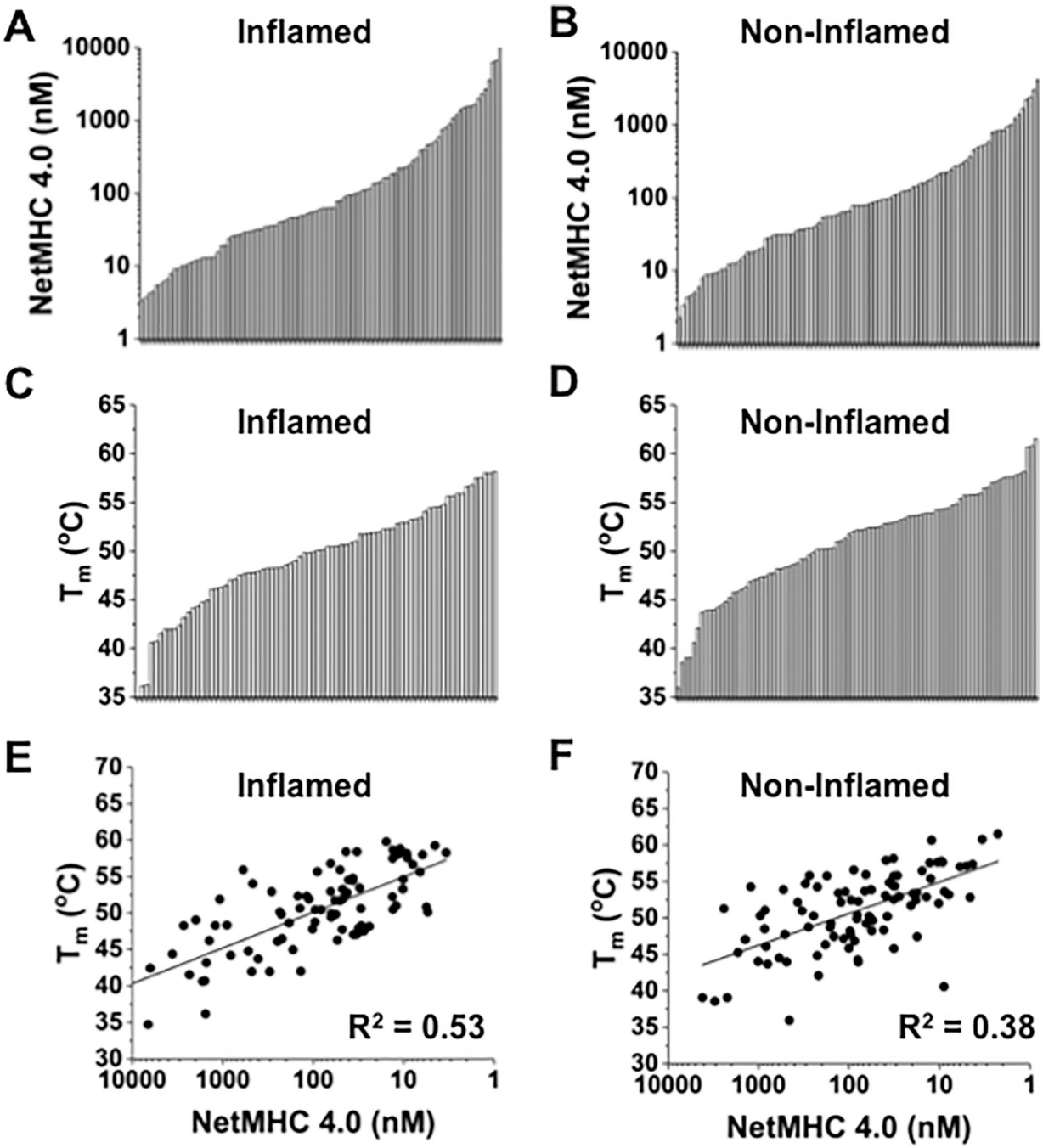

Figure 6. Analysis of neoantigen/HLA-A2 complexes identified from TCGA.

(A, B) Distribution of NetMHC 4.0 values for HLA-A2-restricted neoantigens from TCGA-indicated inflamed and non-inflamed tumor microenvironments, respectively. **(C, D)** Distribution of T_m values, obtained from DSF, for HLA-A2–restricted neoantigens from inflamed and non-inflamed tumor microenvironments, respectively. **(E)** Relationship (R^2=0.53) between predicted binding affinity and T_m for 85 neoantigens found in inflamed tumor microenvironments. **(F)** Correlation (R^2=0.38) of predicted binding affinity and T_m for 91 neoantigens found in non-inflamed tumor microenvironments. Analysis revealed no

statistically significant difference between T_m values measured for peptides from the two sources (inflamed and non-inflamed). P=0.4 assessed from a single experiment with three replicates of each neoantigen in the inflamed and non-inflamed cohorts, using a two-tailed Student *t* test (t=0.85, two degrees of freedom) with significance accepted at $p<0.05$).

Table 1.

T_m analysis of HLA-A2 complexes containing immunogenic neoantigen peptides

Gene	Sequence	NetMHC 4.0 (nM)	T_m (°C)
Fritsch et al. (32)			
ME-1	FLDEFMEGV	3	63.2 ± 0.4
FNDC3B	VVMSWAPPV	6	61.6 ± 0.6
PRDX5	LLLDDLLVSI	15	55.3 ± 0.7
GAS7	SLADEAEVYL	43	59.2 ± 0.7
KIAA0223	VLHDDLLEA	29	59.7 ± 0.5
GAPDH	GIVEGLITTV	123	58.5 ± 0.6
HSP70	SLFEGIDIYT	18	59.8 ± 0.6
ACTININ	FIASNGVKLV	281	56.9 ± 0.5
HAUS3	ILNAMIAKI	48	56.9 ± 0.2
CSNK1A1	GLFGDIYLAI	21	52.6 ± 0.6
CLPP	ILDKVLVHL	56	57.1 ± 0.4
CDK4	ACDPHSGHFV	14410	59.9 ± 0.3
Robbins et al. (33), Cohen et al. (34), and Prickett et al. (35)			
AHNAK	FMPDFDLHL	6	60.1 ± 0.2
SRPX	TLWCSPIKV	10	63.7 ± 0.1
COL18A1	VLLGVKLFGV	9	60.9 ± 0.3
ERBB2	ALIHHNTYL	18	59.4 ± 0.5
TEAD1	VLENFTIFLV	51	48.2 ± 0.2
TEAD1	SVLENFTIFL	85	55.8 ± 0.2
NSDHL	ILTGLNYEV	8	61.4 ± 0.1
GANAB	ALYGFVPVL	8	61.7 ± 0.2
Durgeau et al. (36)			
CDC37L1	FLSDHLYLV	2	61.8 ± 0.1
FLNA	HIAKSLFEV	22	56.4 ± 0.4
SPOP	FLLDEAIGL	3	60.7 ± 0.1
Ott et al. (12)			
ACPP	VLAKKLKFV	59	56.8 ± 0.7
DCAKD	LLHTELERFL	624	42.9 ± 0.2
CIT	TLLSQVNKV	33	53.2 ± 0.3

HLA-A2-restricted neoantigen peptides, previously reported as immunogenic by various methods, were analyzed using DSF. The gene name, neoantigen sequence, predicted binding affinity using NetMHC4.0, and T_m value with corresponding standard deviation for each complex tested are shown. T_m values represent the average and standard deviation of three replicates in a single experiment.